

Anisotropic ultracold plasma expansion

Rima Mebrek¹, Rachid Fermous² and Mourad Djebli^{1,3} 

¹USTHB, Faculty of Physics, Theoretical Physics Laboratory, B.P. 32 Bab Ezzouar, 16079 Algiers, Algeria

²Faculty of Sciences and Technology, Djilali Bounaama University, Route de Theniet El Had, 44225 Khemis Miliana, Algeria

E-mail: mdjebli@usthb.dz

Received 2 September 2019, revised 12 October 2019

Accepted for publication 14 November 2019

Published 28 January 2020



CrossMark

Abstract

Based on fluid model, the three-dimensional expansion of ultracold plasma is studied. The model considered both thermal pressure and ambipolar potential rising due to the local charge separation. By using isothermal assumption and quasi-neutrality condition, the time dependent asymmetric expansion parametric investigation is conducted for two different ultracold plasma ion species (Sr^+ and Ca^+). It is found that ion temperature, in the range of ultracold limit, did not affect strongly the expanding profile but decreases the expanding density by an amount of $\sim 0.5\%$ to $\sim 7\%$. The ion inertia is also found to enhance the asymmetric aspect of the anisotropic plasma expansion.

Keywords: plasma expansion, anisotropic, quasi-neutral

(Some figures may appear in colour only in the online journal)

1. Introduction

Recent developments have made it possible to form neutral plasmas with thermal energy much less than the energy required to collisionally ionize atom. Indeed, in plasmas of temperature above 300 K thermal energy leads to collisional ionization which sustains the system and prevent recombination that gives rise to neutral gas where collective effect are not important. To achieve neutral plasma state one has to increase the temperature for moderate densities or have a very high densities at low temperatures, not an easy task for laboratory plasmas, particularly when the temperature is less than 10^4 K. However, at temperatures of order one Kelvin, a neutral plasma is produced by photoionization of laser-cooled atoms. First, Rydberg atoms of density in the range 10^6 – 10^{10} cm^{-3} are cooled and confined in a magneto-optic trap. This Rydberg gas is then ionized by applying a delayed electric field leading to the spontaneous production of ultracold-neutral plasma [1–3]. The latter experimentally began at the National Institute of Standards and Technology since 1999 [1], where ions of temperature ≈ 10 μK had been produced by the photoionization of laser-cooled xenon atoms to have a neutral plasma of density 10^9 cm^{-3} . In such a plasma particles can be near the strongly coupled regime [4, 5]. This

is characterized quantitatively by the Coulomb coupling parameter $\Gamma_x = (Z_x^2 e^2 / 4\pi\epsilon_0 a_x) / k_B T_x$ where, $a_x = (4\pi n_x / 3)^{-1/3}$ is the Wigner–Seitz radius characterizing the separation between particles at density n_x and of temperature T_x . A plasma is said to be in strongly coupled regime when $\Gamma > 1$. Because electron temperature is almost always greater than that of ions, electrons can be in a weakly coupled regime while ions are strongly coupled [6]. Thus, ultracold plasma may span a wide range of applications such as the formation of antihydrogen atoms [6], stopping highly charged ions to be used in trap measurement and diagnostic purposes [7, 8] as well as in the development of plasma based accelerators [9].

Ultracold neutral plasma expansion is mainly governed by electron thermal pressure which makes it very sensitive to electron temperature [10]. To study particles dynamics and energy flow associated to an expanding ultracold plasma, a radio frequency electric field has been used to excite plasma oscillation [11]. Direct imaging of the plasma has also been a very important tool to investigate the plasma expansion [12]. During expansion ions can be removed from the plasma by three body recombination in which one ion and two electrons are involved. An electron and an ion recombine and a second electron serves to conserve energy and momentum resulting on electron and exited atom [3, 13]. This recombination also decreases electron correlation [14]. In the case of freely

³ Author to whom any correspondence should be addressed.

expanding neutral ultracold plasma the strongly coupled parameter increases considerably, due to ions adiabatic cooling [15]. The ion temperature decreases, as the system is not connected to any energy reservoir. For electrons, disorder induced heating leads to a non self-similar expansion in the strongly coupled regime [16] and the quasi-neutrality breaks down. Thus, ultracold plasma expansion evolves a change imbalance leading to slowdown the outer plasma expansion [17]. However, expansion remains self similar despite a non global thermal equilibration. As the neutrality of ultracold plasmas is not perfect, their exterior region, due to electron screening, exhibits a non neutrality which turns out to increase the electron cooling rate [18].

To investigate the spatial expansion of ultracold plasma an isothermal self-similar model has been used. For an elliptical symmetric plasma, the anisotropic expansion is characterized by a faster velocity in the symmetric plan compared to the elongated direction, parallel to the laser probe [19]. Commonly in plasmas ion acceleration can be attributed to thermal processes induced by temperature gradients and to the electric processes resulting from local charge separation. From a theoretical point of view, each processes have their own signatures, especially during the earlier times of expansion. The main aim of the present work is studying the anisotropic ultracold plasma expansion to depict the contribution of both thermal pressure and local charges separation on different directions of the expanding plasma mechanisms. For this purpose the study is conducted to find the main physical parameters that govern such an expansion.

2. Physical model

The laser ionization creates a plasma from where electrons, having enough kinetic energy to overcome the electric barrier, escape leading to a net positive space charge. Then, electrons at the head of expanding front pull ions, by the ambipolar electric field, to be accelerated. Escaping electrons leave the sample within nanosecond time scale [20]. At each point in time these electrons are assumed to be in thermal equilibrium, governed by Maxwell–Boltzmann distribution i.e.

$$n_e(\vec{r}, t) = n_{oe} \exp\left(\frac{e\phi(\vec{r})}{k_B T_e}\right), \quad (1)$$

where $\phi = \phi(\vec{r})$ stands for the electrostatic potential, n_{oe} is the initial electron density, T_e is the electron temperature and k_B is the Boltzmann’s constant. Since the electron thermalization time (\sim ns) is very small compared to the time scale of the ultracold plasma expansion (\sim μ s) [12], electron thermal equilibrium is set during all the process. For an asymptotic behavior i.e. long times the hole plasma expansion is quasi-neutral and self-similar. Thus, the dynamic of the collisionless ions can be described by the following equations,

$$\frac{\partial n_i}{\partial t} + \nabla(n_i v_i) = 0 \quad (2)$$

$$\frac{\partial v_i}{\partial t} + v_i \nabla v_i = -\frac{e}{m_i} \nabla \phi - \frac{1}{n_i m_i} \nabla p_i, \quad (3)$$

where $n_i = n_i(\vec{r}, t)$, $v_i = v_i(\vec{r}, t)$ are the ion density and ion velocity, respectively. m_i , e are the ion mass and the elementary charge, respectively. The set of equations is closed by Quasi-neutrality condition which occurs in plasma expansion as long as the characteristic plasma size is greater than the Debye length. In this case, expansion can be studied without solving Poisson’s equation since we have $\nabla^2 \phi = 0$ and the electrostatic potential $\phi(x)$ can be obtained implicitly from the condition $n_i = n_e$. Such an assumption has been largely used in plasma expansion and provides simple solutions to the expansion problems [21]. Moreover, by using quasi-neutral condition asymptotic solution can be obtained for the sake of solving boundary value problems or combine this solution with other models such as a Child–Langmuir model [22]. Quasi-neutrality applies also for ultracold plasmas where two region are observed, an interior region of the most scientific interest with two-component i.e. ions and electrons, where neutrality applies and a non-neutral outer region. The expansion is very sensitive to the neutrality of the UCP that needs to be considered for correct measurements [18]. However, when the quasi-neutrality breaks down one has to consider non-neutral plasma and solve Poisson’s equation by invoking molecular dynamics or particle-in-cell simulation. From Maxwell–Boltzmann distribution given by equation (1), the electrostatic potential can be written in terms of density and temperature as

$$\phi(\vec{r}) = \frac{k_B T_e}{e} \ln\left(\frac{n_e}{n_{e0}}\right). \quad (4)$$

We note that there is no sink/source terms in equation (2) because we assume that recombination can be neglected and the number is conserved. Indeed, the three-body recombination rate is proportional to $n_e^2 T_e^{-9/2}$. For a plasma of density $\sim 10^{10} \text{ cm}^{-3}$ and electron temperature $\sim 100 \text{ K}$, one finds a rate of $\sim 10^7 \text{ Hz}$ and a corresponding time of $\sim 0.1 \text{ ns}$, very small compared to the expansion time scale [13]. The amount of recombination and its influence strongly depends on the initial electron temperature and density. If the electrons are too hot (about 50 K for typical experimental densities of 10^9 cm^{-3}), recombination is strongly suppressed [23]. In our works we take the temperature 100 K for Ca^+ ion plasma and 55 K of Sr^+ .

Commonly, as the temperature is very small, momentum equation includes only the charge separation effect. The main aim of the present work is to establish the temperature limits for which pressure term has no effect on the ultracold plasma expansion. We use isothermal fluid model [24], where the pressure corresponds to $p_i = k_B T_i n_i$. The three-dimensional plasma expansion results from an initial cylindrical plasma shaped by Gaussian laser. This profile is obtained by adjusting the laser-cooling parameters and imaging the cloud in two perpendicular axes. The initial ion-density distribution is proportional to the Gaussian distribution of the laser-cooled atom cloud from which the plasma is created [16, 25]. The longitudinal direction belongs to the laser propagation axis

and the radius is in the (x, y) plan [20]. However, for an elliptical symmetry the plasma expands in two dimensions. In this case the density drops more slowly than in the three-dimensional case. We hypothesize a density distribution of the form:

$$n_i(x, y, z, t) = \frac{N_i \beta_1 \beta_2^{1/2}}{\pi^{3/2}} \times \exp[-(x^2 + y^2)\beta_1(t) - z^2\beta_2(t)], \quad (5)$$

where N_i is the number of ionized ions and the functions β_1 and β_2 are time dependent. At initial time $\beta_1(0) = \sigma_0^{-2}$ and $\beta_2(0) = \alpha^{-2}\sigma_0^{-2}$. The ions density of $n_i \sim 10^{10} \text{ cm}^{-3}$ results from a laser pulse of intensity about 20 Mw cm^{-2} [12].

Following the change of variables, the ion velocity has a linear form given by [19],

$$\vec{v}_i = \gamma_1(t)(x\vec{i} + y\vec{j}) + \gamma_2(t)z\vec{k}. \quad (6)$$

The plasma is set to be globally neutral throughout the expansion, the quasi-neutrality equation is given by

$$n_e(\vec{r}, t) = n_i(\vec{r}, t). \quad (7)$$

From these assumptions, the electric potential of ultracold plasma can be calculated and expressed as:

$$\phi(x, y, z) = -\frac{k_B T_e}{e}(\beta_1 x^2 + \beta_1 y^2 + \beta_2 z^2). \quad (8)$$

Inserting equation (6), (5) into (2), we obtained the following system of equations

$$\frac{d\beta_k}{dt} = -2\beta_k(t)\gamma_k(t) \quad (k = 1, 2). \quad (9)$$

γ_k is a parameter determining the local mean of the velocity distribution. All components have the same form of solution. By using equations (3)–(6) and (8), one obtains

$$\frac{d\gamma_k}{dt} + \gamma_k^2(t) = \frac{2k_B}{m_i}(T_e + T_i)\beta_k(t). \quad (10)$$

By using equations (9) and (10) we obtain the differential equation

$$\frac{\ddot{\beta}_k}{\beta_k^2} - \frac{3}{2} \frac{\dot{\beta}_k^2}{\beta_k^3} + 2v^2(\lambda + 1) = 0 \quad (11)$$

which describes the dynamic of plasma, where $\lambda = T_i/T_e$, and $v^2 = 2k_B T_e/m_i$ represents the plasma expansion velocity. Solving equation (11) yields main insights into ultra-cold plasma dynamics, through the functional form of the ion expansion,

$$\beta_1(t) = [\sigma_0^2 + (\lambda + 1)v^2 t^2]^{-1} \quad (12)$$

$$\beta_2(t) = [\alpha^2 \sigma_0^2 + (\lambda + 1)v^2 t^2]^{-1} \quad (13)$$

$$\gamma_1(t) = (\lambda + 1)v^2 t \beta_1(t) \quad (14)$$

$$\gamma_2(t) = (\lambda + 1)v^2 t \beta_2(t), \quad (15)$$

where σ_0 being the size of the plasma cloud assumed to be the same as the pulse beam focused to the MOT [26]. The parameter α defines ellipticity of the system [19]. The time evolution of the parameters describing the expansion of an ultracold plasma can be written as

$$n_i(x, y, z, t) = \frac{N_i}{\pi^{3/2}} \frac{(\alpha^2 \sigma_0^2 + (\lambda + 1)v^2 t^2)^{-1/2}}{(\sigma_0^2 + (\lambda + 1)v^2 t^2)} \times \exp \left[-\frac{(x^2 + y^2)}{(\sigma_0^2 + (\lambda + 1)v^2 t^2)} - \frac{z^2}{(\alpha^2 \sigma_0^2 + (\lambda + 1)v^2 t^2)} \right] \quad (16)$$

$$\vec{v}_i = (\lambda + 1)v^2 t \left[\frac{x}{(\sigma_0^2 + (\lambda + 1)v^2 t^2)} \vec{i} + \frac{y}{(\sigma_0^2 + (\lambda + 1)v^2 t^2)} \vec{j} + \frac{z}{(\alpha^2 \sigma_0^2 + (\lambda + 1)v^2 t^2)} \vec{k} \right]. \quad (17)$$

3. Results and discussion

Expansion occurs when a confined fluid finds free openings. It can hold into vacuum or other medium under thermal pressure for a neutral gas and due to the combined effect of thermal pressure and electrostatic potential for a plasma partially or totally ionized. However, an ultracold plasma, is mostly in strongly coupled regime where electric interaction dominates thermal ion agitation. Thus, it is reasonable to question to what extent an ultracold plasma can be assumed only governed by the rise of a local charge separation that creates the ambipolar electrostatic potential. For that purpose in figure 1 is plotted the density variations in the plan x - y for an ultracold plasma. In this figure we have gathered three situations for the expansion mechanism: (a) due to electron thermal pressure (b) with only ion thermal pressure and (c) in the presence of both effects. This is achieved by setting initial ion temperature to zero (non zero ion temperature), initial electron temperature to zero (non zero ion temperature), and then neither temperature to zero, respectively. As reported by previous works [25], ion pressure term did not play a significant role in the ultracold plasma expansion mechanism. Rather, the electrostatic potential (due to electron thermal pressure) that have the main role. Such a potential is created by electron fast motion under electron thermal pressure. As shown by figure 1 profiles are not affected by the presence of ion thermal pressure term in the equation of motion. Such a term reduces the density by an amount of 0.5% at the plasma bulk, where the density is high and the particle inter-distance is small. The ion pressure term contribution is more important at the plasma outer-shells where the plasma is rarefied to give a density reduction by an amount of $\sim 7\%$ on the density when ion thermal pressure is considered. In the plan x - y , the expanding profiles remain symmetric whatever the processes. However, by analyzing different expansion mechanisms its clear that under electron thermal pressure effect the expansion is faster. At the first stage light-weighted species and higher speed electrons are at the head of the expanding front and pull

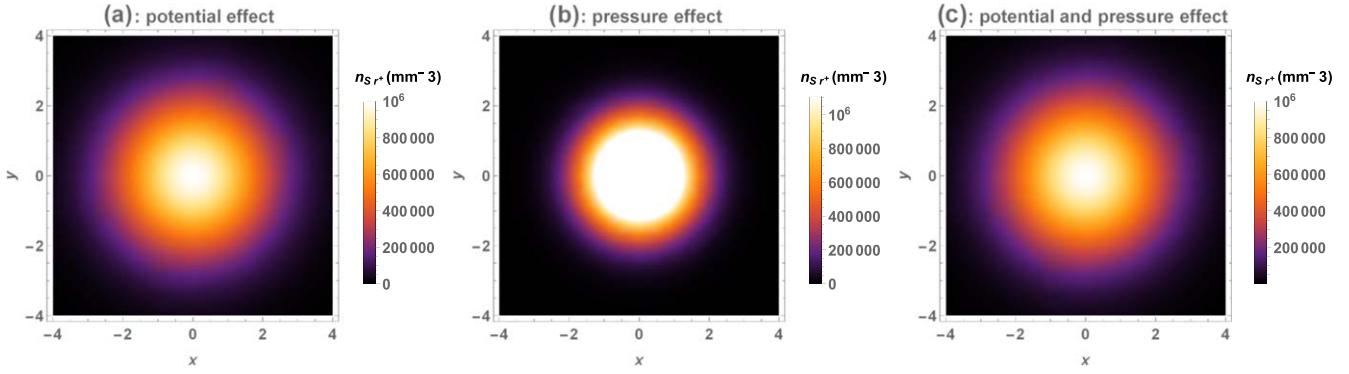


Figure 1. Plots of Sr^+ ion density measured in the x - y plan at a fixed expansion time corresponding to $t = 10^{-5}$ s. Initial parameters correspond to $\sigma_o = 1.4$ mm, $T_i = 1$ K, $T_e = 55$ K [27]. (a) In the presence of only the electrostatic term, (b) under the effect of thermal pressure and (c) in the presence of both electrostatic and thermal pressure effects.

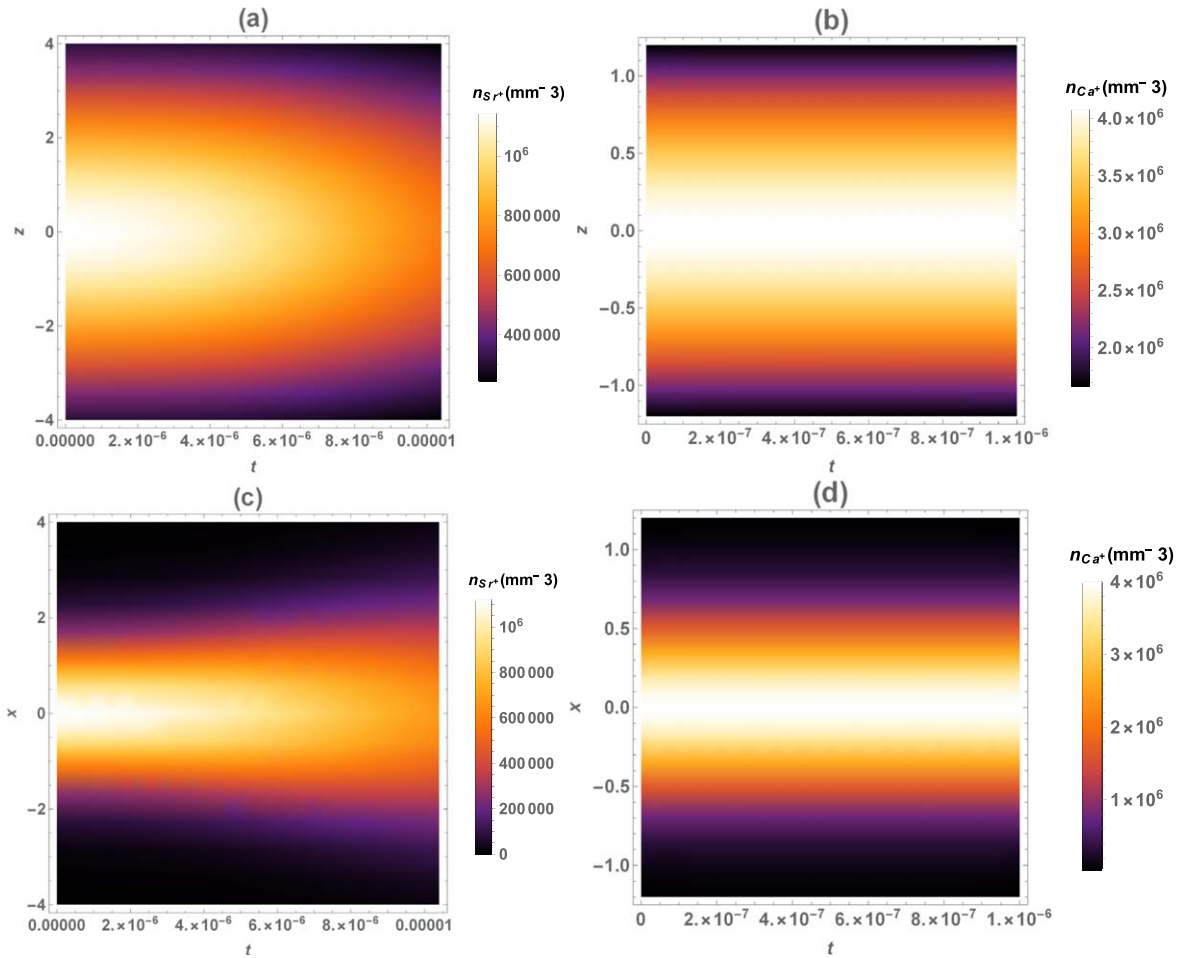


Figure 2. Contour plot of plasma density variation during a specific time domain. (left) for Sr^+ in the domain $t \in [0, 10^{-5}]$ s and right for Ca^+ in the domain $t \in [0, 10^{-6}]$ s. First row in z direction and the second row corresponds to x direction.

with them some ions to preserve quasi-neutrality. Thus, these ions slow-down the next wave expanding ions (of the inner shell) which, at the end, makes all the expanding processes slower.

In figure 2, the first row is plotted by considering $\alpha = 2.5$, $\sigma_o = 1.4$ mm, $T_i = 1$ K, $T_e = 55$ K and ion number $N_i = 7 \times 10^7$ ([12, 27]) for Sr^+ and for the second row we use $\sigma_o = 0.05$ cm, $N_i = 10^5$ and $T_e = 100$ K with Ca^+ as an

ion species [24]. Note that the expanding domain is not the same because light-weighted ultracold plasma ion species finds its expansion ends earlier ($n \rightarrow 0$). As the initial ion distribution was set asymmetric, this is preserved during all the expansion time. However, the asymmetric behavior is stronger for heavy ion species (Sr^+), may be due to particles inertia which force the Gaussian profile as the system expands and governs the dynamics. The energy is localized in the

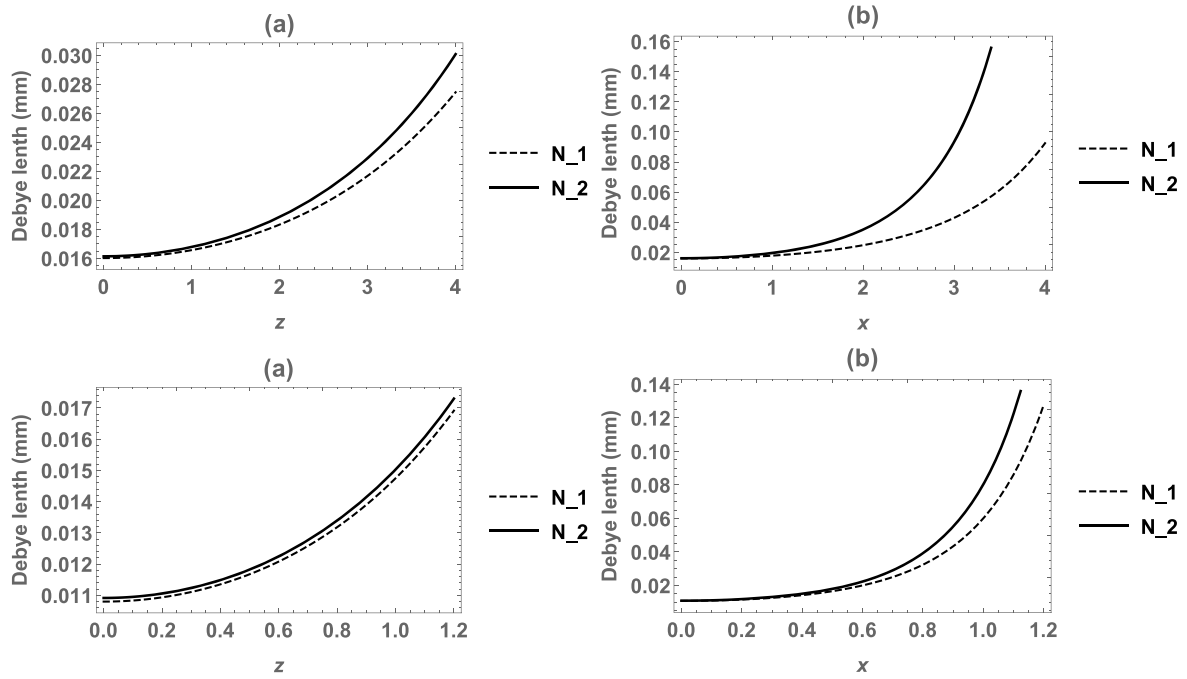


Figure 3. Debye length versus z (a) and versus x (b). First row for Sr⁺ ions with initial ionized atoms number $N_1 = 9.9 \times 10^7$ and $N_2 = 5.13 \times 10^7$ and second row for Ca⁺ with initial ionized atoms number $N_1 = 8 \times 10^6$ and $N_2 = 6 \times 10^6$.

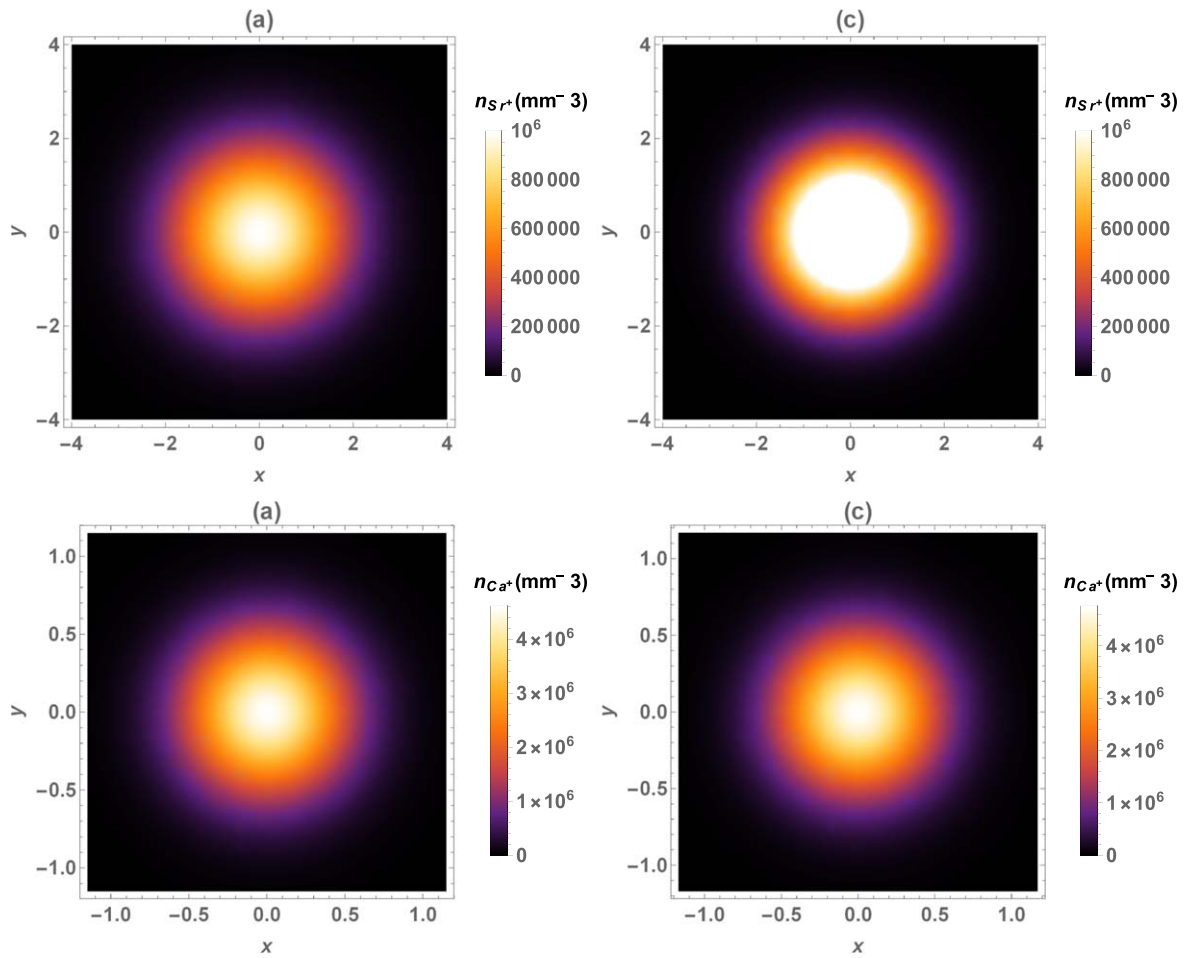


Figure 4. Initial velocity effect on ion density. First row for Sr⁺ and second row for Ca⁺. Initial velocities $v = 50$ (a) and 100 (c) m s⁻¹ [28].

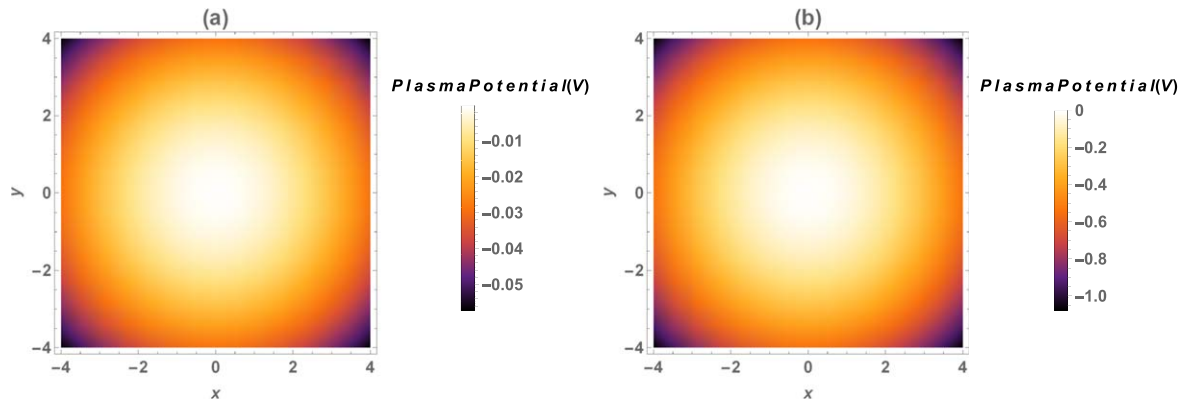


Figure 5. Expansion velocity effect on plasma potential for $v = 80 \text{ m s}^{-1}$ (b). First row for Sr^+ and second row for Ca^+ .

plasma bulk ($z \sim 0$), ions of this region have sufficient energy to overcome the coulomb barrier but faster for light-weighted species which turns to give similar profiles in x and z directions. Indeed, although the expansion is self-similar because the Debye length remains less than the plasma size (figure 3) it grows faster for Sr^+ and particularly in the z -direction to reach the present model limitation (quasi-neutral assumption).

In figure 4 we investigated the effect of initial velocity on radial expansion. This velocity is achieved by the outward electron pressure [28] which is monitored by electron temperature. In a recent work [29] the electron temperature was found to play a crucial role due to diverse heating and cooling mechanisms in which they are involved. The acceleration of electrons having higher kinetic energy turns to increase the local ambipolar potential giving rise to faster ion motion of the outer shell, as shown by the second column of figure 4. In addition, This leads immediately to a stronger field which keep a higher density in the bulk plasma particularly when the ion inertia is weak because of the strongly coupling between particles (figure 5). Thus, initial expansion velocity can be used to monitor the density [30].

4. Conclusion

The three-dimensional expansion of a laser-produced ultracold plasma having a Gaussian shape is studied using a fluid model for ions along with isothermal electrons having asymmetric Gaussian distribution characterized by time dependent parameters. In the quasi-neutral limit, numerical investigation showed that the ultracold ion expansion is governed by the ambipolar potential created by local charge separation rather than ion thermal pressure which only reduces the density of the expanding front by an amount ranging from $\sim 0.5\%$ for the bulk plasma to $\sim 7\%$ for the plasma outer-shells. However, the electron temperature which governs the initial velocity of the expansion has a significant effect on the time expansion evolution. In addition the inertia effect investigated by studying the expansion of ultracold plasma of Sr^+ (heavy-weighted) as ion species and light-weighted one (Ca^+) reveals that the asymmetric aspect of the expansion is stronger when the ion inertia is important.

ORCID iDs

Mourad Djebli  <https://orcid.org/0000-0001-6882-8945>

References

- [1] Killian T C, Kulin S, Bergeson S D, Orozco L A, Orzel C and Rolston S L 1999 *Phys. Rev. Lett.* **83** 4776–9
- [2] Robinson M P, Tolra L, Noel M W, Gallagher T F and Pillet P 2000 *Phys. Rev. Lett.* **85** 4466–9
- [3] Killian C, Lim M J, Kulin S, Dumke R, Bergeson S D and Rolston S L 2001 *Phys. Rev. Lett.* **86** 3759–62
- [4] Simien C E, Chen Y C, Gupta P, Laha S, Martinez Y N, Mickelson P G, Nagel S B and Killian T C 2004 *Phys. Rev. Lett.* **92** 143001
- [5] Chen Y C, Simien C E, Laha S, Gupta P, Martinez Y N, Mickelson P G, Nagel S B and Killian T C 2004 *Phys. Rev. Lett.* **93** 265003
- [6] Mendonça J T and Terças H 2013 *Physics of Ultra-Cold Matter: Atomic Clouds, Bose–Einstein Condensates and Rydberg Plasmas* (New York: Springer)
- [7] Deutsch C, Zwignagel G and Bret A 2009 *J. Plasma Phys.* **75** 799–815
- [8] Bussmann M, Schramm U and Habs D 2006 *Hyperfine Interact.* **173** 27–34
- [9] Cianchi A et al 2018 *Phys. Plasmas* **25** 056704
- [10] Wilson T, Chen W T and Roberts J 2013 *Phys. Plasma* **20** 073563
- [11] Kulin S, Killian T C, Bergeson S D and Rolston S L 2000 *Phys. Rev. Lett.* **85** 318–21
- [12] Killian T C, Pattard T, Pohl T and Rost J M 2007 *Phys. Rep.* **449** 77–130
- [13] Robicheaux F and Hanson J D 2002 *Phys. Rev. Lett.* **88** 055002
- [14] Sadeghi H, Schulz-Welling M, Yin J, Saquet N, Rennick C and Grant E 2011 *Phys. Chem. Chem. Phys.* **13** 18872
- [15] Phol T, Pattard T and Rost J M 2005 *Phys. Rev. Lett.* **95** 205003
- [16] Gupta P, Laha S, Simien C E, Gao H, Castro J, Killian T S and Pohl T 2007 *Phys. Rev. Lett.* **99** 075005
- [17] Chen T, Lu R, Guo L and Han S 2016 *Phys. Plasmas* **23** 092102
- [18] Witte C and Roberts J L 2014 *Phys. Plasmas* **21** 103513
- [19] Cummings E A, Daily J E, Durfee D S and Bergeson S D 2005 *Phys. Plasmas* **12** 123501
- [20] Comparat D, Vogt T, Zahzam N, Mudrich M and Pillet P 2005 *Mon. Not. R. Astron. Soc.* **361** 1227–1242f
- [21] Mora P 2003 *Phys. Rev. Lett.* **90** 185002

- [22] Degong P, Parzani C and Vignal M H 2003 *Multiscale Model. Simul.* **2** 158–78
- [23] Pohl T, Pattard T and Rost J M 2004 *Phys. Rev. A* **70** 033416
- [24] Cummings E A, Daily J E, Durfee D S and Bergeson S D 2005 *Phys. Rev. Lett.* **95** 235001
- [25] Laha S, Gupta P, Simien C E, Gao H, Castro J, Pohl T and Killian T C 2007 *Phys. Rev. Lett.* **99** 155001
- [26] Twedt K A 2012 Electron distribution and electrostatic oscillation of an ultracold plasma *PhD Dissertation*
- [27] McQuillen P, Castro J, Strickler T, Bradshaw S J and Killian T C 2013 *Phys. Plasma* **20** 043516
- [28] Fletcher R S, Zhang X L and Rolston S L 2006 *Phys. Rev. Lett.* **96** 105003
- [29] Jiang P and Roberts J L 2019 *Phys. Plasmas* **26** 043513
- [30] Roberts J L, Fertig C D, Lim M J and Rolston S L 2004 *Phys. Rev. Lett.* **92** 253003